AAPS PharmSciTech (2021) 22: 68
DOI: 10.1208/s12249-021-01938-7

Research Article

Physicomechanical, stability, and pharmacokinetic evaluation of aceclofenac dimethyl urea cocrystals

Hafsa Afzal,[1,2] Nasir Abbas,[1] Amjad Hussain,[1] Sumera Latif,[2] Kanwal Fatima,[1] Muhammad Sohail Arshad,[3] and Nadeem Irfan Bukhari[1,4]

Received 7 September 2020; accepted 15 January 2021; published online 9 February 2021

Abstract. Poor physicomechanical properties and limited aqueous solubility restrict the bioavailability of aceclofenac when given orally. To improve its above properties, aceclofenac (ACE) was cocrystallized with dimethyl urea (DMU) in 1:2 molar ratio by dry and solvent assisted grinding. The cocrystals were characterized by ATR-FTIR, DSC, and PXRD, and their surface morphology was studied by SEM. There was enhancement in intrinsic dissolution rate (IDR) (~eight- and ~fivefold in cocrystals prepared by solvent assisted grinding (SAG) and solid state grinding (SSG), respectively, in 0.1 N HCl, pH 1.2) and similarly (~3.42-fold and ~1.20-fold in phosphate buffer, pH 7.4) as compared to pure drug. Additionally, mechanical properties were assessed by tabletability curves. The tensile strength of ACE was < 1 MPa in contrast to the cocrystal tensile strength (3.5 MPa) which was ~1.98 times higher at 6000 psi. The tablet formulation of cocrystal by direct compression displayed enhanced dissolution profile (~36% in 0.1 N HCl, pH 1.2, and ~100% in phosphate buffer, pH 7.4) in comparison to physical mixture (~ 30% and ~ 80%) and ACE (~18% and ~50%) after 60 min, respectively. Stability studies of cocrystal tablets for 3 months indicated a stable formulation. Pharmacokinetic studies were performed by using rabbit model. The $AUC_{0-\infty}$ (37.87±1.3 μgh/ml) and C_{max} (6.94±2.94 μg/ml) of the selected cocrystal C1 prepared by SAG were significantly enhanced ($p < 0.05$) and were ~3.43 and ~1.63-fold higher than that of ACE. In conclusion, new cocrystal of ACE-DMU was successfully prepared with improved tabletability, *in vitro* and *in vivo* properties.

KEY WORDS: aceclofenac; dimethyl urea; cocrystals; intrinsic dissolution rate; mechanical properties; stability; *in vitro* dissolution; *in vivo* bioavailability.

INTRODUCTION

Optimization of physicochemical, mechanical, and pharmacokinetic attributes is strategically crucial in the course of development of the physical form of an active pharmaceutical ingredient (API) in which it is to be administered (1). Since 80% of the developed drug candidates seem to have solubility problem and belong to BCS class II (less soluble, high permeable) (2), so their oral absorption is limited (3–6). There are various strategies for improvement of solubility, dissolution, and bioavailability like microfluidic, spray drying, electrosprayed mesoporous particles, and inorganic drug delivery systems (7). In addition to these approaches, the solid form modification of APIs (salt formation, polymorphs, and cocrystals) is of considerable significance for addressing the poor solubility of drugs. Since amorphous forms are thermodynamically unstable, salt formation is limited to ionizable compounds (8). In comparison to the above, crystal engineering finds substantial significance in tailoring the physicochemical and pharmaceutical properties of drugs, particularly those belonging to BCS class II (9–12). Pharmaceutical cocrystallization is considered to be an attractive alternative in modification of properties of the existing solid form of an API (6). Apart from improvement in physicochemical properties like solubility and dissolution, pharmaceutical cocrystals can also modify other fundamental properties of APIs such as flowability, compressibility, stability, and pharmacokinetics (13–16). Pharmaceutical cocrystals are the multicomponent systems comprising two or more molecular moieties, i.e., API and the pharmaceutically acceptable molecule (coformer or

[1] Punjab University College of Pharmacy, University of the Punjab, Allama Iqbal Campus, Lahore, 54000, Pakistan.
[2] Institute of Pharmacy, Faculty of Pharmaceutical and Allied Health Sciences, Lahore College for Women University, Jail Road, Lahore, Pakistan.
[3] Department of Pharmacy, Bahauddin Zakariya University, Multan, Pakistan.
[4] To whom correspondence should be addressed. (e–mail: nadeem_irfan@hotmail.com)

cocrystal coformer) in precise stoichiometric proportion, bonded together by means of freely reversible, non-covalent, or nonionic interactions (17–19).

Aceclofenac (ACE), belonging to BCS class II, is an orally effective non-steroidal anti-inflammatory drug, broadly used for its remarkable analgesic properties in rheumatoid arthritis, osteoarthritis, and ankylosing spondylitis (20). Being a weekly acidic drug (pKa = 4–5), it exhibits pH-dependent solubility and absorption. Due to insufficient solubility in gastrointestinal environment, it leads to many *in vitro* and *in vivo* upshots such as inadequate release from the dosage form, decreased bioavailability, and high intra- and inter-subject variability when given orally (21). Moreover, its slight water solubility (58μg/ml) (22) leads to its exacerbating side effects related to gastrointestinal tract.

The ACE is marketed as a neutral drug due to its degradation in strongly acidic and basic media (23), unlike the other members of this class (diclofenac and indomethacin), which are marketed as sodium or potassium salt, respectively, ACE is marketed as a neutral drug. The presence of proton donor and the acceptor sites in ACE has made it a good candidate for cocrystallization by using appropriate coformers. Therefore, there is a potential for addressing and modulating the pharmaceutical and pharmacokinetic properties of this poorly soluble drug**.**

Among the several selected coformers, cinnamic acid is a common pharmaceutically acceptable coformer in cocrystal studies (24). Amides (benzamide) are often used as coformers for pharmaceutical multicomponent system (25,26). The 1,3 dimethyl urea (DMU), a derivative of urea, is a hydrophilic agent used for synthesis of caffeine and pharmaceuticals, (27). The DMU has potential to form intermolecular hydrogen bonds due to the presence of amide as functional group, thus could be used as conformer. DMU has been reported to stabilize the metastable, form of antitubercular drug, pyrazinamide for many years by spray drying (28). However, DMU has not been reported earlier as a coformer in cocrystallization. In the present work, an attempt was made to develop cocrystals of ACE with improved physicochemical and mechanical behavior. The prepared cocrystals were formulated into tablet by direct compression. Pharmacokinetic studies of the developed cocrystals were performed by using rabbit model.

EXPERIMENTAL

Materials

ACE, sodium starch glycolate, and magnesium stearate were obtained as gift samples from Highnoon Laboratories Lahore, Pakistan. DMU, cinnamic acid, and benzamide were procured by Sigma-Aldrich, Pakistan. Avicel PH 102 was obtained as gift sample form Remington pharmaceuticals, Lahore, Pakistan. All other organic solvents and chemicals used were of HPLC or analytical grade.

Preparation of Cocrystals

Solid State Grinding (SSG)

ACE and three coformers, cinnamic acid, benzamide, and 1,3 DMU in different molar ratios (1:1, 1:2, 2:1), were separately ground in pestle and mortar for 30 min. The physical mixtures (PMs) were prepared by mixing of the drug with the above coformers, using the same ratios. The samples were stored in air tight jars for further characterization.

Solvent-Assisted Grinding (SAG)

Drug and coformers in abovementioned ratios were ground followed by addition of 100 μl of ethanol for each 100 mg of powder sample for 30 min. The samples produced from SAG were stored in air tight containers for further characterization. Same method was used for the preparation of PMs.

Solvent Evaporation (SE)

ACE and coformer in same molar ratios as above were dissolved in ethanol and acetonitrile separately with slight heating till the formation of a clear solution. The solutions were filtered (0.45 μm) and left for evaporation at 25°C, 30% humidity. The solid obtained after slow evaporation of the solvent was stored in air tight jars for further studies.

Solid State Characterization

ACE, coformers, and all the samples prepared by the above methods were analyzed by powder X-ray diffraction, DSC-TGA, ATR-FTIR, SEM, and intrinsic dissolution rate (IDR) studies.

Differential Scanning Calorimetry (DSC)

DSC was carried out by using a TA instrument (model Q, USA) having standard aluminum pan with an empty pan as reference. Samples (2−5 mg) were heated ranging from room temperature (25± 2°C) to 300°C at a rate of (10°C/min).

Powder X-Ray Diffraction (PXRD)

PXRD pattern from the powdered samples without any. pretreatment was recorded. The data was collected by using wide angle diffractometer (Bruker) (operating at 40 kV, 40 mA), using Cu-Kα radiation (λ = 1.5418 Å) keeping step dimension of 0.02° in 2 θ range of 5–40°.

ATR-FTIR

Fourier transform infrared spectra (FTIR) were obtained for ACE, DMU, and the prepared cocrystals using FTIR (Alpha-P Bruker, Germany) equipped with an ATR unit. The measurements were recorded across the range of 400–3500 cm^{-1}.

Scanning Electron Microscopy (SEM)

Images of powder samples were photographed by Carl Zeiss Microscopy Cambridge C B 1, 3JS (Carl Zeiss, NTS Ltd., Cambridge, UK) with auto imaging system. The samples were mounted on carbon adhesive tape fixed on aluminum stubs.

Intrinsic Dissolution Rate (IDR)

Using the static disk method, the IDR of the ACE, prepared cocrystals, and PM were studied under sink conditions in 0.1 N HCl, pH 1.2, and phosphate buffer, pH 7.4 (16). The sample powders (300) mg were compressed at 6000 psi pressure for 2 min on a hydraulic tablet press (Carver Inc., USA). The compressed disks were covered with paraffin wax, exposing only a plane surface with 13 mm diameter for estimation of dissolution. The disk was immersed in 900 ml of dissolution medium in USP type-II apparatus, operated at 50 rpm at 37°C. The samples were drawn at preset time intervals: 0, 25, 50, 75, 100, 200, 300, 400, 500, 600, 700, 800, and 900 min in 0.1 N HCl and 0, 2, 4, 6, 8, 10, 12, 14, 16, 18, 20, 22, 24, and 26 min in phosphate buffer, pH 7.4. The different time intervals were taken due to difference in solubility of ACE in both media. The sink conditions were maintained by restocking the withdrawn amount with the equal amount of blank. All the samples were filtered through 0.45 μm filter, and UV absorption was measured at λ_{max} 273 to quantify the amount of ACE in both media (29). The total amount of drug dissolved per surface area (mg/cm^2) was plotted against time (min) for the calculation of IDR.

Micromeritics and Tableting Performance

To investigate the impact of cocrystallization on material flow characteristics, the micromeritic properties of the cocrystals were also studied by standard methods for determination of bulk and tapped densities, angle of repose, Carr's index, and Hausner's ratio.

The Compaction/Mechanical Properties

Tablets of each pure substance (300 mg) were prepared without any excipient under six different compaction pressures (1000–6000 psi) using hydraulic press (Carver, USA) equipped with flat faced dies having 13mm diameter at 21°C and 30% RH (30). Tablet thickness, diameter, and weights were determined. The breaking force, F in Newton (N), was measured by employing Pharmatron Multitest 50H hardness tester. Tensile strength, σ, in MPa was determined by using equation (31).

$$\sigma = \frac{2F}{10^6 \pi DT}$$

where D is the tablet diameter (m), T symbolizes thickness of tablet (m), and σ is the tensile strength in (MPa). The tabletability profile was determined by plotting tablet tensile strength against compaction pressure.

Formulation of Tablets

On the basis of highest IDR value, the tablet formulation (F1) of the selected cocrystal was developed by direct compression approach. For this purpose, weight of cocrystal sample equivalent to 100 mg of ACE was taken. To this, Avicel PH 102 (25% of cocrystal weight), sodium starch glycolate (4% of cocrystal weight), and magnesium stearate (0.3% of cocrystal weight) were added. The formulation of PM (F2) in was developed in the similar way. For comparison, formulation of pure ACE (F3) was developed by adding starch powder (20% to the weight of ACE) as a diluent. Rest of the excipients and quantities were same as in other formulations. All the materials were passed through sieve # 40 and thoroughly mixed for 15 min. Magnesium stearate was added in the end, and the mixture was again blended for another 2 min. Compression of tablets were achieved by using hydraulic press as described above.

Evaluation of Formulated Tablets

All tablets were evaluated for average weight, thickness, diameter, and hardness. The disintegration time was determined as specified in *British Pharmacopoeia 2010*.

In Vitro Drug Release Study

In vitro drug release was studied in 900 ml of 0.1N HCl, pH 1.2, and phosphate buffer, pH 7.4, by using USP type-II apparatus with paddle speed at 50 rpm. Aliquots (5ml) were drawn at preset time intervals: 0, 25, 50, 75, 100, 150, 200, 250, 300, 350, and 400 min for 0.1 N HCl and 0, 5, 10, 15, 20, 25, 30, 35, 40, 45, 50, 55, and 60 min for the phosphate buffer. The sink conditions were preserved by replenishing the same amount with the withdrawn amount of the dissolution media. Rest of the sample treatment was the same as carried out for the samples in IDR measurement. All the measurements were done in triplicate.

Preliminary Stability Studies

The cocrystal-based formulation F1 and pure ACE formulation F3 were subjected to preliminary stability studies for the period of 3 months under normal conditions (25°C/60% RH) and at accelerated conditions (40°C/75% RH) (32,33).

***In Vivo* Studies**

Rabbits weighing 1.75–2.00 kg of either sex, divided into two groups, each comprising six rabbits, were used for pharmacokinetic study. All the protocols of the study were endorsed by animal ethical committee, University College of Pharmacy, University of the Punjab, Lahore, Pakistan, vide reference number, D/705/UZ dated 05/03/2020. Prior to experimentation, the rabbits were acclimatized (in cages) one week at 25 ± 5°C with 12 h light/12 h dark cycle with free access to food and water. Before the experiment, all the animals were fasted for 12 h with only access to water. A dose of 10 mg/kg body weight for pure ACE and equivalent cocrystal filled in the hard gelatin capsules (# 5) was given

Table I. Screening of ACE with DMU

Methods	Solvent used	Molar ratio of ACE/DMU	Cocrystal formation
Solvent assisted grinding (SAG)	Ethanol	1:1	-
	Acetonitrile	1:2	+ C1
		2:1	-
Solid state grinding (SSG)		1:1	-
		1:2	+ C2
		2:1	-
Solvent evaporation (SE)	Ethanol	1:1	-
	Acetonitrile	1:2	-
		2:1	-
		1:1	-
		1:2	-
		2:1	-

+ represents the formation of cocrystals. The codes C1 and C2 are given to the successful cocrystals formed by solvent assisted grinding and solid state grinding, respectively

with 10–12 ml of water, to two groups of rabbits (34). Blood samples (1 ml) were withdrawn from the jugular vein of the animals in heparinized tubes at 0.0, 0.5, 1.0, 1.5, 3.0, 6.0, 9.0, and 12.0 h post dose intervals. The plasma was immediately separated by centrifugation at 4000 rpm for 5 min in Eppendorf tube and stored at −20°C for further study.

Plasma Sample Treatment

The plasma stored at −20°C was thawed at room temperature and vortexed for 1 min. To 500 µl of plasma, 500µl of acetonitrile was added. The resultant solution was again vortexed for 5 min and centrifuged at 10,000 rpm for 10 min. The supernatant was separated and filtered through 0.22-µm syringe filter. The clear filtrate consisting of 20µl was injected into the HPLC. The total run time of the sample was 12 min. The drug content was analyzed with the previously reported method (35). Plasma drug concentration was determined by HPLC system Shimadzu 20A, Japan. The equipment consisted of LC-20AT VP pump, a SIL-20AC HT auto sampler, CMB 20A controller unit having a reverse phase symmetry C18 (4.6 × 250 mm, 5-µm particle size). The analysis was done under isocratic conditions keeping the column at 40°C by using CTO 20 AC column oven. The mobile phase was comprised of acetonitrile: deionized water (55:45) with pH adjusted to 2.8 by orthophosphoric acid, filtered through 0.45-µm membrane filter, and injected at the flow rate of 1ml/min. The chromatograms were recorded at 273 nm by using SPD-M20A photodiode array detector set at 273 nm. The calibration curve $R^2 = 0.998$ was constructed for ACE, depending on the measurement of peak area of standard solutions and their respective spiked plasma samples for concentrations 0.5, 1.0, 2.0, 5.0, 10.0, and 15.0 µg/ml. The LOQ and LOD were 0.1 and 0.03 µg/ml, respectively.

The peak plasma concentration (C_{max}) and the time to reach $C_{max,}$ (T_{max}) were directly obtained from the plasma concentration versus time curve. The other pharmacokinetics parameters including area under the curve (AUC), mean residence time (MRT), clearance (CL), apparent volume of distribution (Vd), elimination rate constant (K_{el}), and the half-life ($t_{1/2}$) were calculated using non-compartmental analysis implemented in PKSolver (version 2.0) program (36). The data was analyzed statistically by using Mann Whitney test employing SPSS (IBM SPSS Statistics 21). A p value less than 0.05 was used as significant.

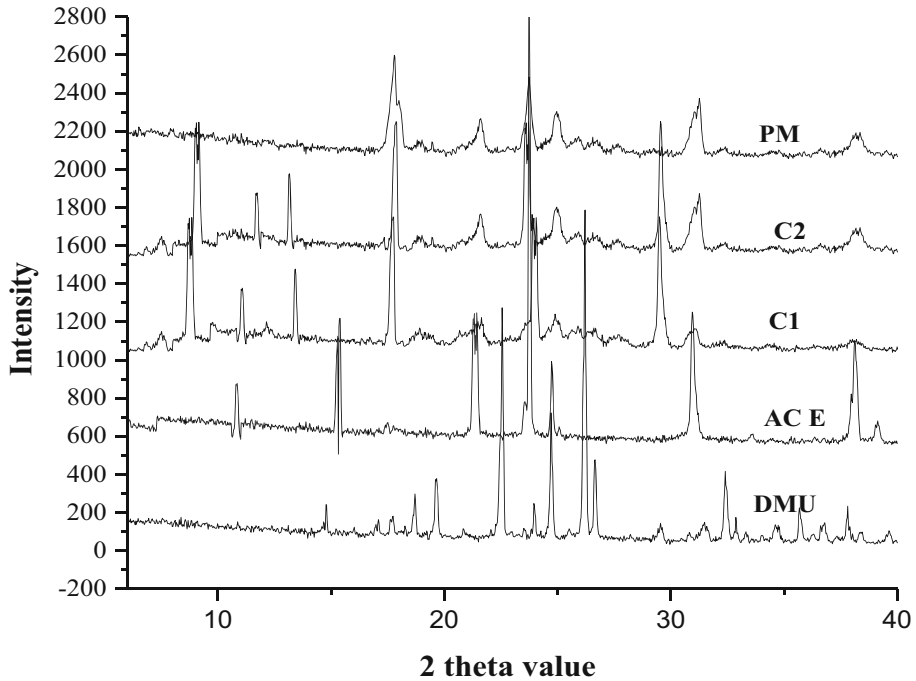

Fig. 1. Comparison of PXRD pattern of DMU, ACE, C1, C2, and PM

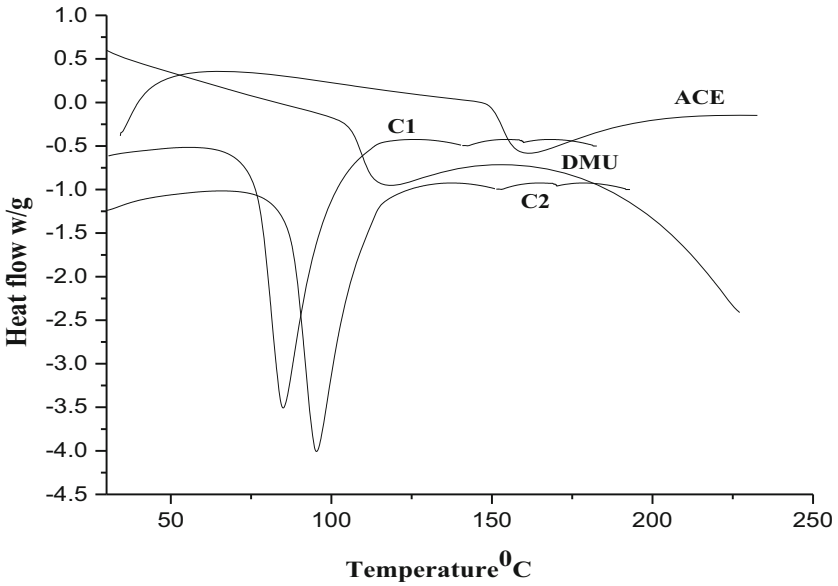

Fig. 2. Comparison of DSC thermogram of DMU, ACE, C1, and C2

RESULTS AND DISCUSSION

Primarily, we selected three coformers, namely, cinnamic acid, benzamide, and dimethyl urea in an attempt to form cocrystals of aceclofenac in 1:1, 1:2, and 2:1 molar ratio by mechanochemical (solid state grinding (SSG) and solvent assisted grinding (SAG)) and solvent evaporation approach. The initial characterization was based on the measurement of melting point and DSC**.** Benzamide and cinnamic acid did not proved to be prolific coformers. This might be due to the presence of the bulky phenyl group in both coformers which imparts steric hindrance, making them more difficult to pack in multicomponent system (26).

The dimethyl urea was the only successful coformer which resulted in formation of cocrystal with ACE in 1:2 molar ratio by mechanochemical approach, i.e., by solvent assisted grinding (SAG) and solid state grinding (SSG). As coherent with the recently reported literature, it has been observed that mechanochemical synthesis was also found to be successful in cocrystallization of aceclofenac with l-cysteine (37). The data on screening with DMU has been included in the text as Table I.

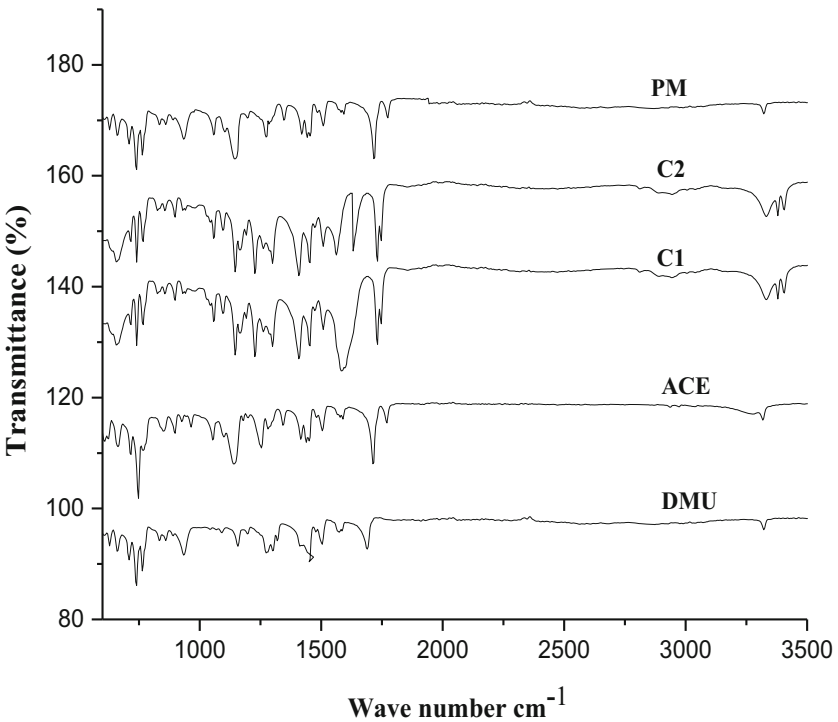

Fig. 3. Comparison of ATR-FTIR spectra of DMU, ACE, C1, C2, and PM

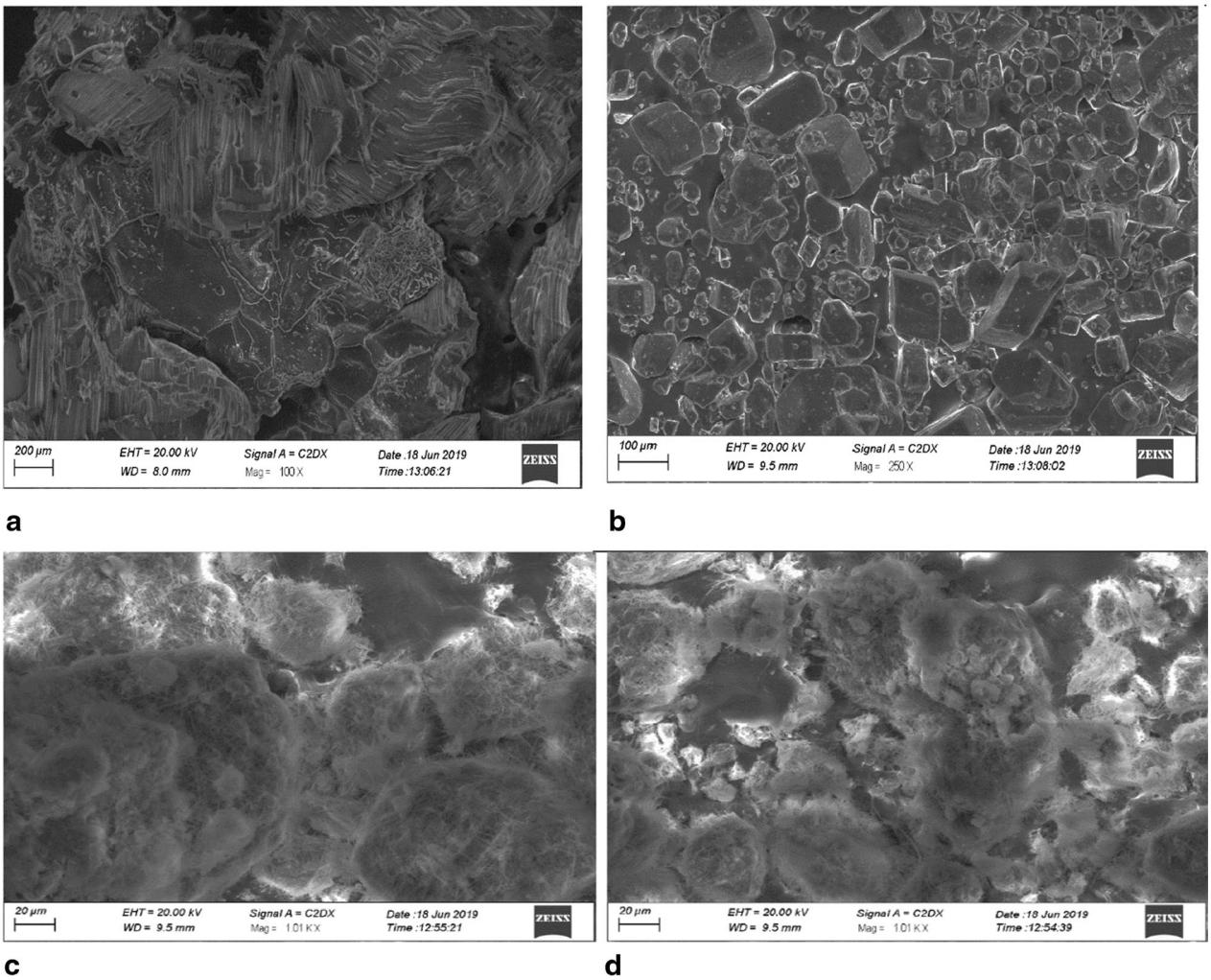

Fig. 4. SEM microphotograph of **a** DMU, **b** ACE, **c** C1, and **d** C2

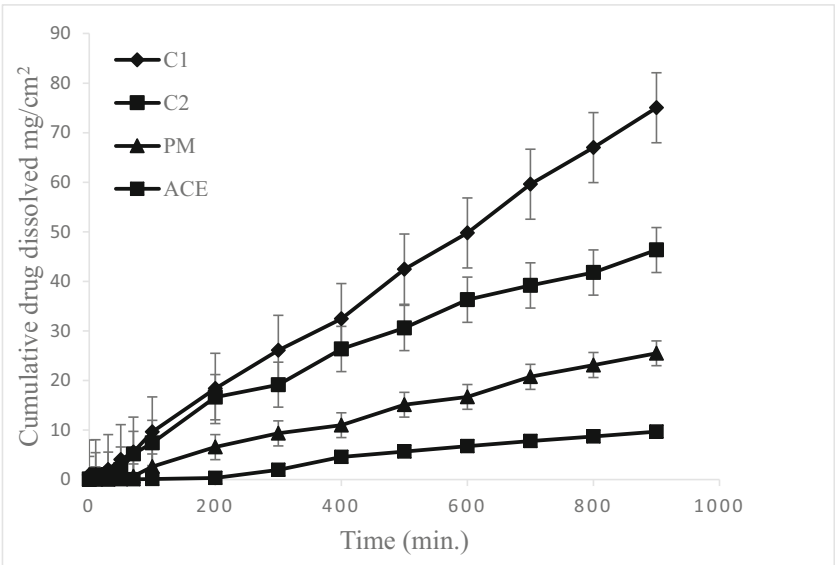

Fig. 5. Intrinsic dissolution profile of cocrystals C1, C2, PM, and ACE in 0.1 N HCL, pH 1.2, at 37°C (n=6)

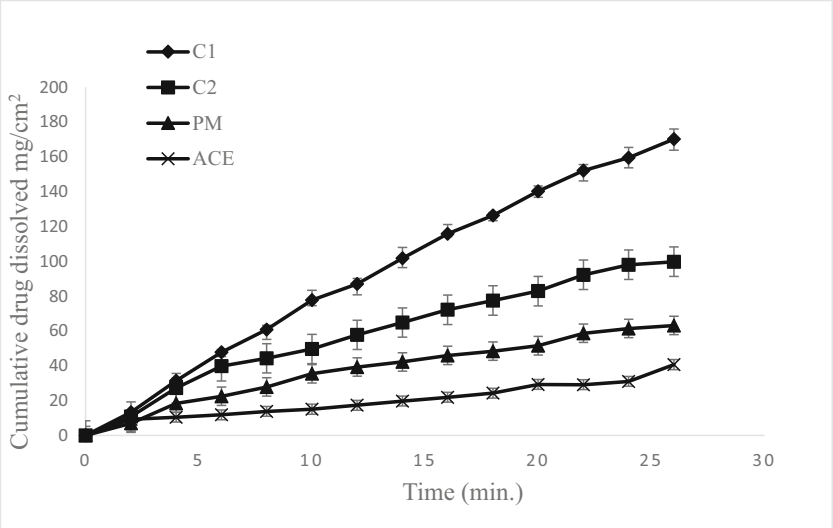

Fig. 6. Intrinsic dissolution profile of cocrystals C1, C2, PM, and ACE in phosphate buffer pH 7.4 at 37°C (n=6)

Among the several methods for cocrystal formation, the mechanochemical approach is more vibrant in preparing cocrystals of APIs with different coformers. This method is more reliable, green, convenient, and cost-effective for new crystalline forms discovery (38). In SSG, the energy needed to complete cocrystallization is lacking, whereas in SAG, the covalent interactions between the components may be induced which offers enhanced selectivity (39). Moreover, in SAG, the presence of solvent acts as catalyst to mediate the reaction kinetics by wetting the solid surfaces and helps in the formation of cocrystals. The SAG has also been reported as an efficient cocrystal screening method in comparison to solution crystallization. On the other hand, cocrystal formation by solvent evaporation is not always successful. For cocrystallization by solvent evaporation, the starting materials must be soluble in a common solvent. The difference in the solubility of initial components leads to the recrystallization of a single material. Furthermore, the cocrystal formation is dependent on the nucleation. The process of nucleation depends on the rate of evaporation of the solvent. The rate of solvent evaporation is significantly dependent on the experimental conditions (40). However, literature has shown that cocrystals with higher solubility than the pure solid form often do not result from solvent evaporation technique (41).

Characterization of Cocrystals

The primary technique for cocrystal detection is PXRD, as the phase changes can directly be observed by changes in pattern. PXRD pattern for ACE alone, DMU, and PM (1:2) and cocrystals C1 and C2 are depicted in Fig. 1. In consistence with the literature, ACE showed specific diffraction peaks at 2θ value of 10.79°, 21.00°, 23.74°, 24.75°, and 31.00° (20).

Likewise, the characteristic reflection pattern of DMU was observed at 2θ value of 14.80°, 18.70°, 19°, 22.00°, 24.00°, and 26.00°. The PXRD pattern of the PM demonstrated the combined pattern of original components depicting absence of any phase change. The characteristic diffraction pattern of ACE and DMU was not observed in ACE-DMU cocrystals prepared by both methods. Moreover, new peaks of C1 were emerged at 2θ value of 8.90°, 11.00°, 13.00°, 17.00°, and 21.43° and for cocrystal C2 at 2 θ of 9.13°, 11.73°, 13.13°, 17.50°, and 21.60°.

The dissimilar PXRD pattern of the cocrystals from their starting materials might suggest the formation of new phases (42). Furthermore, the relative intensities of their PXRD pattern were also varied. The almost similar reflection patter of the two cocrystals might suggest the phase purity of the new phases.

DSC is a rapid screening tool for cocrystal characterization. The energy needed to overcome attractive forces which holds the crystal structure is its melting point (43,44). Figure 2 depicts the DSC curves of ACE, DMU, and cocrystals C1 and C2. The DSC curve of ACE and DMU showed a single endothermic peak at 156.43°C and 107°C, respectively, while ACE-DMU cocrystals (C1 and C2) showed single endothermic peaks at 88.30°C and 94.84°C, respectively, which is lesser than either of its starting materials, signifying the formation of cocrystals. It has also been observed that the cocrystals are not undergoing any phase transitions before and after the single endothermic peak over the entire temperature range which denotes lack of polymorphism.

As per reported data on cocrystals, only half of the cocrystals have shown the melting point between the initial components, and 39% of the reported cocrystals have melting points lower than their initial components. Also, the melting

Table II. Comparison of Micromeritic Properties of ACE and C1

Micromeritic property	ACE	C1
Bulk density (g/cm^3)	0.29±0.019	0.34±0.016
Tapped density (g/cm^3)	0.38±0.021	0.41±0.011
Angle of repose	40.25°±0.43	22.12±0.32
Hausner's ratio	1.65	1.32
Carr's index (%)	36.48	10.36

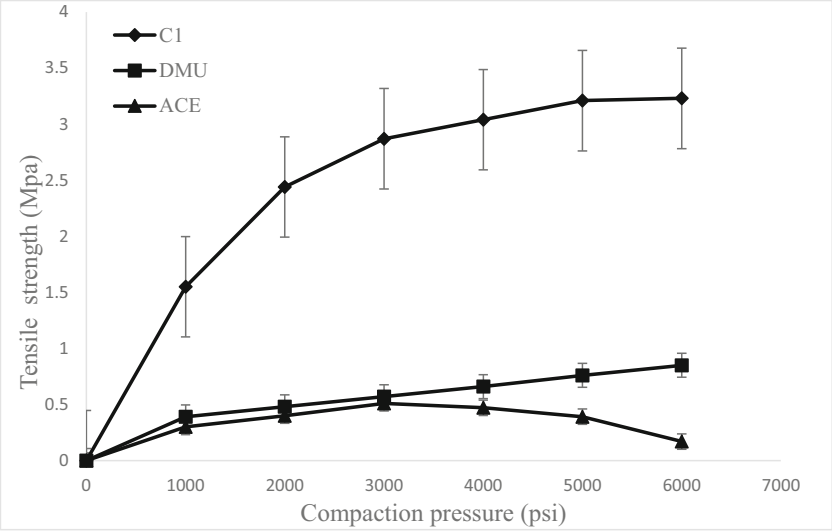

Fig. 7. Tabletability plots of C1, DMU, and ACE (n=6)

point of cocrystals depends on the melting points of the selected coformer (14).

The difference in melting points of the two cocrystals from the starting materials may reflect the change in crystal lattice, of the cocrystals as evident from SEM images (Fig. 4) which in turn be responsible for difference in their physico-chemical properties like solubility and dissolution (45). The changes in these parameters may refer to the alteration in the thermodynamic stability. Crystals with greater hydrogen bonding or molecular symmetry tend to show higher melting points (44). Else ways better dissolution could be displayed by low melting point cocrystals.

The FTIR spectrum for the ACE, DMU, C1, and C2 was recorded in the spectral range of 400–3500 cm^{-1} as illustrated in Fig. 3. In the IR spectra of ACE, a number of peaks were observed at different prominent places showing the presence of functional groups. The peak found at 1579.45 cm^{-1} was due to C–C stretch, whereas peaks at 1250, 1500, and 1716.59 were due to C=O stretching, which indicated the presence of carboxylic group and keto functional groups. The infrared band appearing at 3333.23 cm^{-1} in ACE and at 3329.45 cm^{-1} in DMU was assigned to NH_2 functional group. The presence of these peaks confirms the purity of drug sample. Whereas cocrystals C1 and C2 showed a distinctive spectrum, especially the peaks attributed to C=O stretch of the carboxylic acid has been shifted to 1163, 1568, and 1728 cm^{-1}, respectively, whereas the peak assigned to NH_2 functional group has appeared at 3380.41 cm^{-1} in comparison to the starting components. The shift in the position and intensity of these peaks could be attributed to the formation of new hydrogen bonding pattern in cocrystals. However, the IR spectrum of PM resembled that of pure DMU and ACE.

The shape and surface morphology of ACE, DMU, and the cocrystals C1 and C2 are presented in Fig. 4. The SEM microphotographs showed that pure ACE and DMU exists in large crystals, while C1 was needle-shaped aggregates while C2 were aggregates. The difference in morphology has resulted by the solvent assisted grinding. This change may influence the nature of bulk particle such as flow properties, bulk density, compressibility and dissolution behavior of the cocrystal (46).

Table III. Physical Parameters of Formulations Prepared from F1 (C1), F2 (PM), and F3 (ACE) (n=6)

Parameters	F1	F2	F3
Weight (mg)	200±0.13	200±0.51	200±0.26
Thickness (mm)	4±0.2	4±0.1	4±0.5
Diameter (mm)	9±0.6	9±0.3	9±0.1
Breaking force (N)	196±3	83.1±1.3	34±1.6
Disintegration time (min)	3	2	5

Intrinsic Dissolution Rate

IDR is a promising tool that can be used to assess the dissolution-mediated absorption of the recently developed APIs (47). Moreover, IDR has shown to be in direct proportion to the solubility of the drug, ignoring the complicating factors in powder dissolution studies like particle size, rate of wetting, disintegration, and clumping. Therefore, the solubility can be predicted from the slope of dissolution curve. In context to this, the IDR studies were conducted to determine the influence of cocrystallization on the dissolution behavior of newly synthesized cocrystals. Figures 5 and 6 describe the dissolution profile of C1, C2, ACE, and PM in 0.1N HCl, pH 1.2, and phosphate buffer, pH 7.4. As ACE exhibits pH-dependent solubility and dissolution, the above media were selected to closely relate the pH conditions of GIT, also to study the effect of cocrystallization on dissolution behavior at different pH. The IDR (from 0 to 1000 min) of C1 was 0.08 mg/cm^2 min, and C2 was 0.05 mg/cm^2 min in 0.1 N HCl, pH 1.2, which was ~eight- and ~fivefold higher in comparison to ACE (0.01 mg/cm^2). The PM also displayed gradual rise in IDR (0.026 mg/cm^2 min) which was found to be ~2.6 times higher than ACE. Likewise, the IDR (from 0 to 30 min) displayed by C1 and C2 in phosphate buffer, pH 7.4, was 6.717 mg/cm^2 min and 3.78 mg/cm^2 min, respectively, which was ~ 3.42-fold and ~1.92-fold

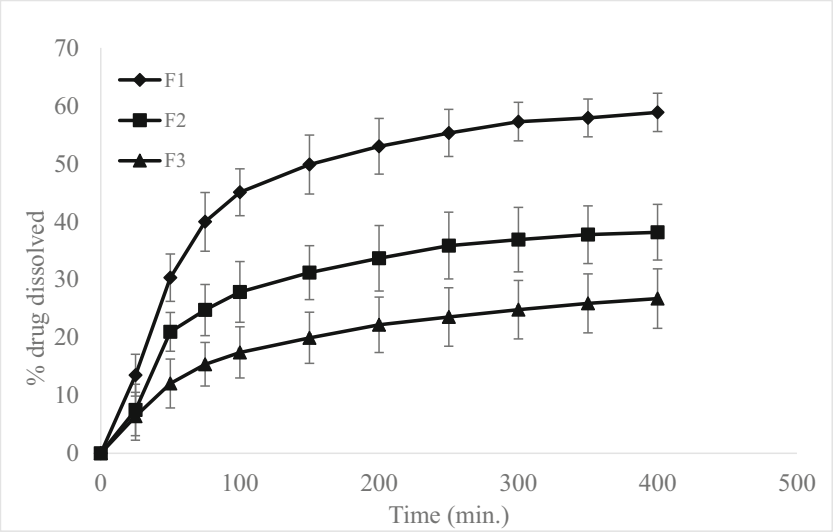

Fig. 8. Comparative *in vitro* drug release from F1 (C1), F2 (PM), and F3 (ACE) formulation in 0.1 NHCl, pH 1.2 (n=6)

higher as compared to ACE (1.96 mg/cm^2 min), whereas the IDR of PM (2.36 mg/cm^2 min) was found to be ~ 1.20-fold higher than ACE.

In our present study, the ACE-DMU exhibited higher dissolution in both acidic and basic media. This was observed in good correlation with the hydrophilic nature of the DMU (water solubility 765 g/ml at 25°C). The pH-dependent changes in the IDR pattern displayed by the cocrystals could be further explained by the changes in the microenvironmental pH of the cocrystal system at the dissolving solid liquid interface (48). The modification of the microenvironmental pH was imparted by the highly water soluble coformer, DMU, which upon ionization in the dissolution medium, presented changes in the pH of the system favoring the dissolution of nonionizable drug. DMU imparted more basic microenvironment to ACE-DMU cocrystal making it even more soluble in the acidic medium (49). The difference in the IDR of cocrystals might be related to the effect of crystal morphology as shown by SEM (Fig. 4).

Micromeritic Properties/Tableting Performance

The micromeritic properties of ACE and C1 have been described in Table II. The improvement in these properties was observed in cocrystals as compared to the ACE.

The cocrystals exhibited improved micromeritic properties in contrast to ACE. The bulk and tapped densities were higher for C1 than ACE which indicated the low porosity of the powder and imparts high compressibility to cocrystal. Lower values of Hausner's ratio and angle of repose for C1 in comparison to ACE reflected good flow characteristics. The suitability of cocrystal powder for direct tableting was also suggested by low Carr's index values in contrast to ACE.

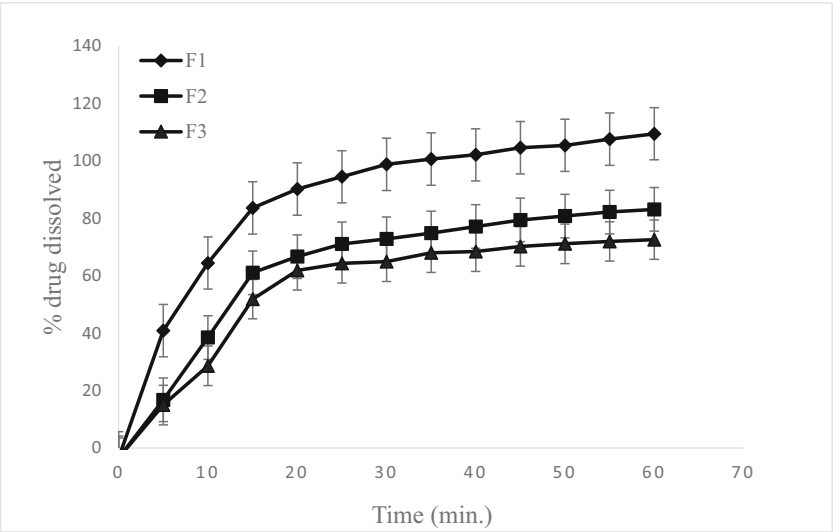

Fig. 9. Comparative *in vitro* drug release from F1 (C1), F2 (PM), and F3 (ACE) formulation in phosphate buffer, pH 7.4 (n=6)

Table IV. Results of Preliminary Stability Studies of F1 and F3 (n=6)

Formulation	Initial	25 °C/60 % RH (3 months)	40 °C/75%RH (3 months)
F1 (%content)	98.90 ± 1.37	97.65 ± 0.56	96.23 ± 1.90
F3 (% content)	98.78 ± 1.10	97.66 ± 0.34	94.50 ± 1.43

A significant parameter by which the mechanical properties of cocrystals can be determined is the measurement of their tensile strength. In the present work, we studied the tabletability of C1. The impact of compression pressure on the cocrystal tensile strength was more prominent as compared to that on the ACE. The high tensile strength of cocrystal compact subjected to the same compression pressure as ACE compact is evident from Fig. 7. The ~threefold increase in tensile strength of the cocrystal as compared to the pure ACE may be attributed to high plasticity due to the presence of slip mechanism (50,51). The increase in the tensile strength of cocrystal at low compression pressure, i.e., 1 and 2 MPa, may be attributed to larger bonding area between the adjacent cocrystal particles which in turn be responsible for higher tabletability (50). However, the tensile strength of the cocrystal compact was continued to rise with rise in pressure and levelled off gradually which represents the characteristic behavior of plastic materials. Thus, ACE in the form of cocrystal is more suitable for tableting. In case of the pure ACE compact, there was slight increase in tablet tensile strength at 3 MPa. The decline in tensile strength was observed at 4 MPa by increasing the compaction pressure, owing to the low plasticity as well as more elastic recovery of the material. On the other hand, DMU showed a minor linear increase in tensile strength with increasing compaction pressure resembled the characteristic behavior of brittle material.

Evaluation of Formulated Tablets

The tablet formulations based on cocrystal C1 (F1), PM (F2), and ACE (F3) were evaluated in terms of average weight, thickness, diameter, and breaking force as described in Table III. All these parameters were appropriate. The tablet disintegration time of all the formulations was found to be within official limits (B.P).

In Vitro Performance of Tablets

ACE-DMU cocrystals were formulated into tablets by employing direct compression approach without the addition of any binder due to plastic deformation imparted by cocrystallization. The comparison of the pharmaceutical attributes and key parameters of all tablet formulations is shown in Table III. The dissolution studies were conducted in acidic and basic media. Cocrystal C1 was given the formulation code F1 manifested enhanced dissolution profile in both media. The dissolution in 0.1 N HCl was more embolden. More than 50% of the drug was released from F1, within 400 min which was greater than F2 which released only 30% of ACE and F3 manifested only 20% release. This rapid dissolution in the acidic medium could be credited to altered microenvironment pH of the dissolving cocrystal system conferred by the ionizable coformer. There was more than 100% release of ACE from F1 within 30 min in phosphate buffer as compared to the F2 which released 60%, while F3

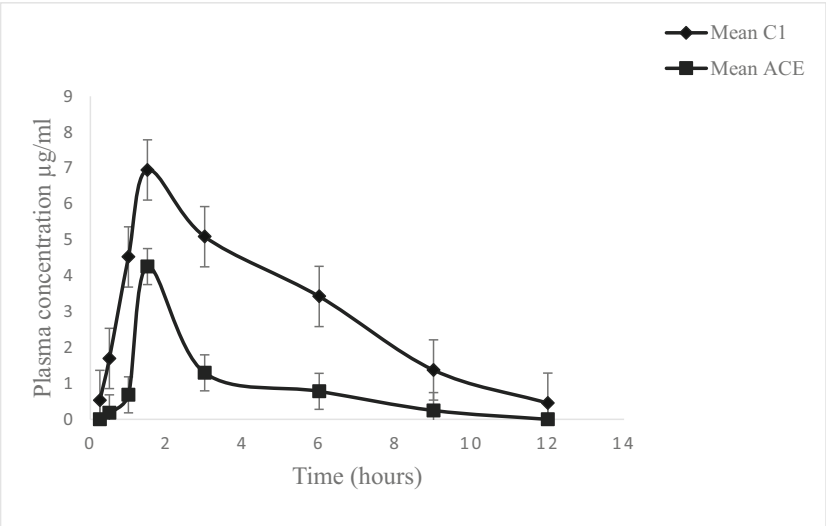

Fig. 10. Rabbit plasma concentration with time for C1 and ACE (n=6)

Table V. Pharmacokinetic Parameters of ACE and C1 in Rabbit, Obtained After Single Oral Administration at the Dose of 10mg/kg (n=6)

Parameters	ACE (mean ± SD)	C1 (mean ± SD)
C_{max} (μg/ml)	4.25±2.05	6.94±2.94
T_{max} (h)	1.5±0.61	1.5±1.31
$AUC_{0\text{-}12}$ (μgh/ml)	4.32±2.9	17.7±0.71
$AUC_{0\text{-}\infty}$ (μgh/ml)	11.01±1.6	37.87±1.3
MRT (h)	1.74±0.71	2.06±0.42
Kel (h^{-1})	0.46±0.21	0.35±0.10
$t_{1/2}$ (h)	1.74±0.71	2.06±0.42
CL/F (μg/ml)/h	1.59±1.4	0.306±0.74
Vd/F (μg/ml)	2.98±1.505	0.844±0.2
*Relative bioavailability		4.09

**RB represents bioavailability relative to ACE*

demonstrated only 45% release. In F3 formulation, starch powder was added as diluent which acts as disintegrant. The results revealed that in spite of adding disintegrant in F3, the formulation F1 worked well for disintegration and dissolution. The enhanced dissolution in acidic medium may shorten the residence time of the drug in the gastric environment leading to retard the irritant effects of ACE (Figs. 8 and 9).

Preliminary Stability Studies

The cocrystal formulation (F1) and pure ACE formulation (F3) were subjected to preliminary stability studies for the period of 3 months**.** The results of stability study are depicted in Table IV. The % contents of ACE were within official limits (95–105%) suggesting the stability of ACE cocrystal tablets under accelerated conditions.

In Vivo Performance of ACE-DMU cocrystals

Bioavailability study of powdered sample of cocrystal C1 and pure drug was conducted in rabbit model. Cocrystal C1 was selected on the basis of enhanced dissolution profile as shown in Figs. 5 and 6, respectively. The plasma concentration vs. time data of ACE and the selected cocrystal was depicted in Fig. 10. The mean pharmacokinetic parameters calculated after the single dose in rabbit model are presented in Table V. The mean $AUC_{0\text{-}\infty}$ (37.87±1.3 μgh/ml) and C_{max} (6.94±2.94 μg/ml) presented by the cocrystal was significantly enhanced than $AUC_{0\text{-}\infty}$ (11.01±1.6) and C_{max} of ACE (4.25 ±2.05), based on the Mann-Whitney test ($p < 0.05$) and were found to be 3.43- and 1.63-fold, respectively, higher than ACE. However, it has been observed that the C_{max} (6.94 ±2.94 μg/ml) of ACE-DMU cocrystals was also found to be ~1.85-fold higher than C_{max} (3.75±0.28 μg/ml) of ACE nanocrystals (33). This could be credited to the enhanced dissolution profile and increase in the extent of absorption of ACE-DMU cocrystals.

The cocrystal and the drug were peaked at 1.5 h, showing no significant change in the time for maximum concentration. The above finding indicated that both rate and extent of absorption of ACE were increased in the form of cocrystal as compared to the drug. The ACE-DMU cocrystal showed significantly better $AUC_{0\text{-}\infty}$ than pure drug which translates the extent of absorption of the cocrystal. In fact the increase in the plasma concentration up to 12 h of the cocrystal as compared to the pure drug could be ascribed to the improved IDR and *in vitro* dissolution of the cocrystals. The increase in C_{max} may also be credited to decrease in elimination of drug from the cocrystal. The increase in $t_{1/2}$ was supported by low clearance values of cocrystals as clearance is credited as an indicator of metabolism. Consequently, the low clearance value for the cocrystal (0.306±0.74 (μg/ml)/h) also supports the above finding. The prolonged half-life may also benefit the anti-inflammatory activity of the drug. However, the low Vd values of cocrystals suggested high plasma concentration of drug in blood rather than in the tissues. Mean residence time, calculated by non-compartmental approach, is a determinant for drug persistence in the body. The MRT of cocrystal was observed with low clearance value, suggesting the presence of drug for a longer period of time in the body. The cocrystal exhibited 4.09-fold enhanced relative bioavailability than the pure ACE. These results are significant due to enhancement in AUC and significant decrease in clearance which may suggest reduction in dose and the avoidance of the side effects. It was evident from the *in vitro* dissolution of the cocrystal tablet formulation that the cocrystal helped in fine-tuning the dissolution behavior of poorly soluble API and in turn enhanced its bioavailability.

CONCLUSION

A cocrystal of ACE with DMU was successfully developed in 1:2 molar ratio, by mechanochemical approach. The cocrystals manifested improved IDR and mechanical behavior. Tablet formulation of the cocrystals was developed by direct compression approach and was found to be stable after 3 months under accelerated conditions. The superior *in vitro* behavior of the cocrystal was also reflected in enhancement of *in vivo* bioavailability. The combination of the above advantages could make the cocrystallization as a promising alternative for drug product development.

ACKNOWLEDGEMENTS

We would like to pay special thanks to Mr. Mohammad Moqeet Khan, from University of Veterinary and Animal Sciences, for his cooperation and help in pharmacokinetic studies.

DECLARATIONS

Competing interests The authors declare no competing interest.

REFERENCES

1. Karagianni A, Malamatari M, Kachrimanis K. Pharmaceutical cocrystals: new solid phase modification approaches for the formulation of APIs. Pharmaceutics. 2018;10(1):18.
2. Loftsson T, Brewster ME. Pharmaceutical applications of cyclodextrins: basic science and product development. J Pharm Pharmacol. 2010;62(11):1607–21.

3. Aakery CB, Salmon DJ. Building co-crystals with molecular sense and supramolecular sensibility. 2005.
4. Childs SL, Zaworotko MJ. The reemergence of cocrystals: the crystal clear writing is on the wall introduction to virtual special issue on pharmaceutical cocrystals: ACS Publications; 2009.
5. Henck J-O, Byrn SR. Designing a molecular delivery system within a preclinical timeframe. Drug Discov Today. 2007;12(5-6):189–99.
6. Friščić T, Jones W. Benefits of cocrystallisation in pharmaceutical materials science: an update. J Pharm Pharmacol. 2010;62(11):1547–59.
7. Sayed E, Haj-Ahmad R, Ruparelia K, Arshad M, Chang M-W, Ahmad Z. Porous inorganic drug delivery systems—a review. AAPS PharmSciTech. 2017;18(5):1507–25.
8. Tong HH, Chow AS, Chan H, Chow AH, Wan YK, Williams ID, et al. Process-induced phase transformation of berberine chloride hydrates. J Pharm Sci. 2010;99(4):1942–54.
9. Datta S, Grant DJ. Crystal structures of drugs: advances in determination, prediction and engineering. Nat Rev Drug Discov. 2004;3(1):42–57.
10. Blagden N, de Matas M, Gavan PT, York P. Crystal engineering of active pharmaceutical ingredients to improve solubility and dissolution rates. Adv Drug Deliv Rev. 2007;59(7):617–30.
11. Desiraju GR. Chemistry beyond the molecule. Nature. 2001;412(6845):397–400.
12. Desiraju GR. Crystal engineering: a brief overview. J Chem Sci. 2010;122(5):667–75.
13. Schultheiss N, Newman A. Pharmaceutical cocrystals and their physicochemical properties. Cryst Growth Des. 2009;9(6):2950–67.
14. Shan N, Perry ML, Weyna DR, Zaworotko MJ. Impact of pharmaceutical cocrystals: the effects on drug pharmacokinetics. Expert Opin Drug Metab Toxicol. 2014;10(9):1255–71.
15. Miroshnyk I, Mirza S, Sandler N. Pharmaceutical co-crystals–an opportunity for drug product enhancement. Expert Opin Drug Deliv. 2009;6(4):333–41.
16. Abbas N, Latif S, Afzal H, Arshad MS, Hussain A, Sadeeqa S, et al. Simultaneously improving mechanical, formulation, and in vivo performance of naproxen by co-crystallization. AAPS PharmSciTech. 2018;19(7):3249–57.
17. Brittain HG. Cocrystal systems of pharmaceutical interest: 2010. Cryst Growth Des. 2012;12(2):1046–54.
18. Arora KK, Zaworotko MJ. Pharmaceutical co-crystals: a new opportunity in pharmaceutical science for a long-known but little-studied class of compounds. Polymorphism in Pharmaceutical Solids: CRC Press. 2018:294–329.
19. Shan N, Zaworotko MJ. The role of cocrystals in pharmaceutical science. Drug Discov Today. 2008;13(9-10):440–6.
20. Sharma G, Saini MK, Thakur K, Kapil N, Garg NK, Raza K, et al. Aceclofenac cocrystal nanoliposomes for rheumatoid arthritis with better dermatokinetic attributes: a preclinical study. Nanomedicine. 2017;12(6):615–38.
21. Usha AN, Mutalik S, Reddy MS, Ranjith AK, Kushtagi P, Udupa N. Preparation and, in vitro, preclinical and clinical studies of aceclofenac spherical agglomerates. Eur J Pharm Biopharm. 2008;70(2):674–83.
22. Vadher AH, Parikh JR, Parikh RH, Solanki AB. Preparation and characterization of co-grinded mixtures of aceclofenac and Neusilin US 2 for dissolution enhancement of aceclofenac. AAPS PharmSciTech. 2009;10(2):606–14.
23. Goud NR, Suresh K, Nangia A. Solubility and stability advantage of aceclofenac salts. Cryst Growth Des. 2013;13(4):1590–601.
24. Wouters J, Rome S, Quéré L. Monographs of most frequent co-crystal formers. Pharmaceutical salts and co-crystals: Royal Society of Chemistry London. 2011:338–82.
25. Seaton CC, Parkin A. Making benzamide cocrystals with benzoic acids: the influence of chemical structure. Cryst Growth Des. 2011;11(5):1502–11.
26. Cysewski P, Przybyłek M, Ziółkowska D, Mroczyńska K. Exploring the cocrystallization potential of urea and benzamide. J Mol Model. 2016;22(5):103.
27. Schlottmann U, Stock B, Chemicals OH. SIDS initial assessment report For SIAM 17. 2005.
28. Baaklini G, Dupray V, Coquerel G. Inhibition of the spontaneous polymorphic transition of pyrazinamide γ form at room temperature by co-spray drying with 1, 3-dimethylurea. Int J Pharm. 2015;479(1):163–70.
29. Moffat AC, Osselton MD, Widdop B, Watts J. Clarke's analysis of drugs and poisons: Pharmaceutical press London; 2011.
30. Chow SF, Chen M, Shi L, Chow AH, Sun CC. Simultaneously improving the mechanical properties, dissolution performance, and hygroscopicity of ibuprofen and flurbiprofen by cocrystallization with nicotinamide. Pharm Res. 2012;29(7):1854–65.
31. Fell J, Newton J. Determination of tablet strength by the diametral-compression test. J Pharm Sci. 1970;59(5):688–91.
32. Lucas TI, Bishara RH, Seevers RH. A stability program for the distribution of drug products. Pharm Technol. 2004;28:68–73.
33. Narayan R, Pednekar A, Bhuyan D, Gowda C, Koteshwara K, Nayak UY. A top-down technique to improve the solubility and bioavailability of aceclofenac: in vitro and in vivo studies. Int J Nanomedicine. 2017;12:4921–35.
34. Jung MS, Kim JS, Kim MS, Alhalaweh A, Cho W, Hwang SJ, et al. Bioavailability of indomethacin-saccharin cocrystals. J Pharm Pharmacol. 2010;62(11):1560–8.
35. Naz A, Beg AE, Ahmed KZ, Ali H, Naz S, Zafar F. Pharmacokinetics study of aceclofenac in pakistani population and effects of sucralfate co-administration on bioavailability of aceclofenac. J Appl Res. 2011;11(1).
36. Zhang Y, Huo M, Zhou J, Xie S. PKSolver: an add-in program for pharmacokinetic and pharmacodynamic data analysis in Microsoft Excel. Comput Methods Prog Biomed. 2010;99(3):306–14.
37. Kumar S, Gupta A, Prasad R, Singh S. Novel aceclofenac cocrystals with l-cystine: virtual coformer screening, mechanochemical synthesis, and physicochemical investigations. Curr Drug Deliv. 2020;17.
38. Weyna DR, Shattock T, Vishweshwar P, Zaworotko MJ. Synthesis and structural characterization of cocrystals and pharmaceutical cocrystals: mechanochemistry vs slow evaporation from solution. Cryst Growth Des. 2009;9(2):1106–23.
39. Jones W, Motherwell WS, Trask AV. Pharmaceutical cocrystals: an emerging approach to physical property enhancement. MRS Bull. 2006;31(11):875–9.
40. Sun S, Zhang H, Xu J, Wang S, Wang H, Yu Z, et al. The competition between cocrystallization and separated crystallization based on crystallization from solution. J Appl Crystallogr. 2019;52(4).
41. Steed JW. The role of co-crystals in pharmaceutical design. Trends Pharmacol Sci. 2013;34(3):185–93.
42. Padrela L, de Azevedo EG, Velaga SP. Powder X-ray diffraction method for the quantification of cocrystals in the crystallization mixture. Drug Dev Ind Pharm. 2012;38(8):923–9.
43. Katritzky AR, Jain R, Lomaka A, Petrukhin R, Maran U, Karelson M. Perspective on the relationship between melting points and chemical structure. Cryst Growth Des. 2001;1(4):261–5.
44. Simperler A, Watt SW, Bonnet PA, Jones W, Motherwell WS. Correlation of melting points of inositols with hydrogen bonding patterns. Cryst Eng Comm. 2006;8(8):589–600.
45. Gao Y, Gao J, Liu Z, Kan H, Zu H, Sun W, et al. Coformer selection based on degradation pathway of drugs: a case study of adefovir dipivoxil–saccharin and adefovir dipivoxil–nicotinamide cocrystals. Int J Pharm. 2012;438(1-2):327–35.
46. Haleblian JK. Characterization of habits and crystalline modification of solids and their pharmaceutical applications. J Pharm Sci. 1975;64(8):1269–88.
47. Qiao N, Li M, Schlindwein W, Malek N, Davies A, Trappitt G. Pharmaceutical cocrystals: an overview. Int J Pharm. 2011;419(1-2):1–11.
48. Ren S, Liu M, Hong C, Li G, Sun J, Wang J, et al. The effects of pH, surfactant, ion concentration, coformer, and molecular

arrangement on the solubility behavior of myricetin cocrystals. Acta Pharm Sin B. 2019;9(1):59–73.
49. Latif S, Ijaz QA, Hameed M, Fatima K, Hussain A, Arshad MS, et al. Improvement of physico-mechanical and pharmacokinetic attributes of naproxen by cocrystallization with L-alanine. J Drug Deliv Sci Technol. 2020;102236.
50. Chang S-Y, Sun CC. Superior plasticity and tabletability of theophylline monohydrate. Mol Pharm. 2017;14(6):2047–55.
51. Chattoraj S, Shi L, Sun CC. Understanding the relationship between crystal structure, plasticity and compaction behaviour of theophylline, methyl gallate, and their 1: 1 co-crystal. Cryst Eng Comm. 2010;12(8):2466–72.